Short-Term Prediction of Medium- and Large-Size Earthquakes Based on Markov and Extended Self–Similarity Analysis of Seismic Data

M. Reza Rahimi Tabar[1,2,a], Muhammad Sahimi[3,b], F. Ghasemi[1,c], K. Kaviani[4,d], M. Allamehzadeh[5,e], J. Peinke[6,f] M. Mokhtari[5,g], M. Vesaghi[1,h], M.D. Niry[1,i], A. Bahraminasab[7,k], S. Tabatabai[8,l], S. Fayazbakhsh[1,m] and M. Akbari[5,n]

[1] Department of Physics, Sharif University of Technology, P.O. Box 11365-9161, Tehran, Iran
[c]f_ghasemi@mehr.sharif.edu, [h]vesaghi@sharif.edu,
[i]mdniry@mehr.sharif.edu, [m]S Fayazbakhsh@mehr.sharif.edu

[2] CNRS UMR 6202,Observatoire de la Côte d'Azur, BP 4229, 06304 Nice Cedex 4, France
[a]rahimitabar@sharif.edu

[3] Department of Chemical Engineering and Material Science, University of Southern California Los Angeles, CA 90089, USA
[b]moe@iran.usc.edu

[4] Department of Physics, Az-zahra University, P.O.Box 19834, Tehran, Iran
[d]kaviani@scintist.com

[5] Department of Seismology, The International Institute of Earthquake Engineering and Seismology, IIEES, P.O. Box 19531, Tehran, Iran
[e]Mallam@iiees.ac.ir, [g]Mokhtari@iiees.ac.ir, [n]mary.Akbari@gmail.com

[6] Carl von Ossietzky University, Institute of Physics, D-26111 Oldendurg, Germany
[f]peinke@uni-olden-burg.de

[7] ICTP, Strada Costiera 11, I-34100 Trieste, Italy
[k]abahrami@ictp.it

[8] Institute of Geophysics,University of Tehran, Iran
[l]S.Tabatai@tabagroup.com

Summary. We propose a novel method for analyzing precursory seismic data before an earthquake that treats them as a Markov process and distinguishes the background noise from real fluctuations due to an earthquake. A short time (on the order of several hours) before an earthquake the Markov time scale t_M increases sharply, hence providing an alarm for an impending earthquake. To distinguish a false alarm from a reliable one, we compute a second quantity, T_1, based on the concept of extended self-similarity of the data. T_1 also changes strongly before an earthquake occurs. An alarm is accepted if *both* t_M and T_1 indicate it *simultaneously*.

Calibrating the method with the data for one region provides a tool for predicting an impending earthquake within that region. Our analysis of the data for a large number of earthquakes indicate an essentially *zero* rate of failure for the method.

1 Introduction

Earthquakes are complex phenomena to analyze. The interaction between the heterogeneous morphology of rock and the mechanism by which earthquakes occur gives rise to distinct characteristics in different parts of the world. Seismic data as time series exhibit complex patterns, as they encode features of the events that have occured over extended periods of time, as well as information on the disordered morphology of rock and its deformation during the time that the events were occuring. It is for such reasons that seismic records appear seemingly chaotic.

Published reports indicate the existence of precursory anomalies preceding earthquakes. The reported anomalies take on many different forms, and contain aspects of seismic wave propagation in rock, and its chemical, hydrological, and electromagnetic properties. The spatio-temporal patterns of seismicity, such as anomalous bursts of aftershocks, quiescence or accelerated seismicity, are thought to indicate a state of progressive damage within the rock that prepares the stage for a large earthquake. Numerous papers have reported that large events are preceded by anomalous trends of seismic activity both in time and space. Several reports also indicate that seismic activity increases as an inverse power of the time to the main event (sometimes referred to as an inverse Omori law for relatively short time spans), while others document a quiescence, or even contest the existence of such anomalies at all [1, 2, 3]. If such anomalies can be analyzed and understood, then one might be able to forecast future large events.

There are two schools of thought on the length of the time period over which the anomalies occur and accumulate. One school believes that the anomalies occur within days to weeks before the main shock, but probably not much earlier [4], and that the spatial precursory patterns develop at short distances from impending large earthquakes. Proponents of this school look for the precursory patterns in the immediate vicinity of the mainshock, i.e., within distances from the epicenter that are on the order of, or somewhat larger than, the length of the main shock rupture.

The second school believes that the anomalies may occur up to *decades* before large earthquakes, and at distances much larger than the length of the main shock rupture, a concept closely linked to the theory of critical phenomena [1, 2, 3] which was advocated [1, 2, 5, 6] as early as 1964 with a report [5] on the pre-monitory increase in the total area of the ruptures in the earthquake sources in a medium magnitude range, documenting the existence of long-range correlations in the precursors (over 10 seismic source lengths) with worldwide similarity. More recently, Knopoff *et al.*[7] reported on the existence of long-range spatial correlations in the increase of medium-range magnitude seismicity prior to large earthquakes in California.

Beginning in the late 1970s, models of rock rupture and their relation with critical phenomena and earthquakes were pursued. Vere-Jones [8] pioneered this approach. Hence, a method for the analysis of the data was introduced

that, for certain values of its parameters, led to a power law (typical of critical phenomena) for the system's time-to-failure. Allègre *et al.* [9] proposed a percolation model of damage/rupture prior to an earthquake, emphasizing the multiscale nature of rupture prior to a critical point which was similar to a percolation threshold [10, 11]. Their model was actually just a rephrasing of the real-space renormalization group approach to the percolation model developed by Reynolds *et al.* [12]. Similar ideas were also explored in a hierarchical model of rupture by Smalley *et al.* [13]. Sahimi and co-workers [14, 15, 16] proposed a connection between percolation, the spatial distribution of earthquakes' hypocenters, and rock's fracture/fault networks.

Sornette and Sornette [17] proposed an observable consequence of the critical point model of Allègre *et al.* [9] with the goal of verifying the proposed scaling laws of rupture. Almost simultaneously, but following apparently an independent line of thought, Voight [18] introduced the idea of a time-to-failure analysis in the form of an empirical second-order nonlinear differential equation, which for certain values of the parameters would lead to a time-to-failure power law, in the form of an inverse Omori law. This failure was used and tested later for predicting volcanic eruptions. Then, Sykes and Jaumé [19] performed the first empirical study to quantify with a specific law an acceleration of seismicity prior to large earthquakes. They used an exponential law to describe the acceleration, and did not use or discuss the concept of a critical earthquake. Bufe and Varnes [20] re-introduced a time-to-failure power law to model the observed accelerated seismicity quantified by the so-called cumulative Benioff strain. Their justification of the power law was a mechanical model of material damage. They neither referred to nor discussed the concept of a critical earthquake.

Sornette and Sammis [21] were the first to reinterpret the work of Bufe and Varnes [20], and all the previous ones reporting accelerated seismicity, within a model in which the occurence of large earthquakes is viewed as a critical point phenomenon in the sense of the statistical physics framework of critical phase transitions. Their model generalized significantly the previous works in that the proposed critical point theory did not rely on an irreversible fracture process, but invoked a more general *self-organization* of the stress field prior to large earthquakes. Moreover, using insights from the critical phenomena, Sornette and Sammis [21] generalized the power-law description of the accelerated seismicity by considering *complex* scaling exponents which result in *log-periodic* corrections to the scaling [21, 22, 23, 24, 25, 26]. Such a generalized power law with log-periodic corrections was shown [27] to describe the increase in the energy that rock releases as it undergoes fracturing. These ideas were further developed by Huang *et al.* [28]. Empirical evidence for these concepts was provided by Bowman *et al.* [29], who showed that large earthquakes in California with magnitudes larger than 6.5 are systematically preceded by a power-law acceleration of seismic activity in time over several decades, in a spatial domain about 10-20 times larger than the impending rupture length (i.e., of the order of a few hundred kilometers). The large event

can, therefore, be viewed as a temporal singularity in the seismic history time series. Such a theoretical framework implies that a large event results from the collective behavior and accumulation of many previous smaller-sized events. Similar analysis was reported by Brehm and Braile [30] for other earthquakes.

The work of Ouillon and Sornette [31] on mining-induced seismicity, and Johansen and Sornette [32] in laboratory experiments, made similar conclusions on systems of very different scales, in good agreement with the scale-invariant phenomenology, reminiscent of systems undergoing a second-order critical phase transition. In this picture, the system is subjected to an increasing external mechanical solicitation. As the external stress increases, micro-ruptures occur within the medium which locally redistribute stress, creating stress fluctuations within the rock. As damage accumulates, fluctuations interfere and become more and more spatially and temporally correlated, i.e., there are more and more, larger and larger domains that are significantly stressed and, therefore, larger and larger events can occur at smaller and smaller time intervals. The accelerating spatial smoothing of the stress field fluctuations eventually culminates in a rupture with a size on the order of the system's size. This is the final rupture of laboratory samples, or earthquakes breaking through the entire seismo-tectonic domain to which they belong. This concept was verified in numerical experiments led by Mora *et al.* [33, 34], who showed that the correlation length of the stress field fluctuations increases significantly before a large shock occurrs in a discrete numerical model.

More recently, Bowman and King [35] argued, based on empirical data, that, in a large domain including the impending major event, and similar to the critical domain proposed in Bowman *et al.* [29], the maximum size of natural earthquakes increases with time up to the main shock. If one assumes that the maximum rupture length at a given time is given by (or related to) the stress field correlation length, then the work of Bowman and King [35] shows that the correlation length increases before a large rupture. Note that Keilis-Borok and co-workers [2] have also repeatedly used the concept of a critical point, albeit in a broader and looser sense than its restricted meaning used in the statistical physics of phase transitions.

So far we have discussed the case in which the stress rate is imposed on a system. The problem is, however, more complex when the strain rate is imposed. In this case, the system may not evolve towards a critical point. A possible unifying view point between the two cases is to study whether the dissipation of energy by the deteriorating system slows down or accelerates. The answer to this question depends on the nature of the external loading (an imposed stress, rather than strain, rate), the evolution of the system and how the resulting evolving mechanical characteristics of the system interacts with the external loading conditions. For a constant applied stress rate, the dissipated energy rate diverges in general in a finite time leading to a critical behavior. For a constant strain rate, on the other hand, the answer depends on the damage law. For the Earth crust, the situation is in between the ideal

constant strain and constant stress loading states. The critical point may then emerge as a mode of localization of a global input of energy to the system.

The critical point approach leads also to an alternative physical picture of the so-called seismic cycle. From the beginning of the cycle, small earthquakes accumulate and modify the stress field within the Earth crust, making it correlated over larger and larger scales. When the correlation length reaches the size of the local seismo-tectonic domain, a very large rupture may occur which, together with its early aftershocks, destroys correlations at all spatial scales. This is the end of the seismic cycle, and the beginning of a new one, leading to the next large event. As earthquakes are distributed in size according to the Gutenberg-Richter law, small to medium-size events are negligible in the energetic balance of the tectonic system, which is dominated by the largest final event. However, they are seismo-active in the sense that their occurrence prepares that of the largest one. The opposite view of the seismic cycle is to consider that it is the displacements of the large-scale tectonic plate which dominates the preparation of the largest events, which can be modelled to first order as a simple stick-slip phenomenon. In that case, all the smaller-size events would be seismo-passive, in the sense that they would reflect only the boundary loading conditions acting on isolated faults without much correlations from one event to the other.

Summarizing, in the critical point approach to earthquakes, as the stress on rock increases, micro-ruptures develop that redistribute the stress and generate fluctuations in it. As damage accumulates, the fluctuations become spatially and temporally correlated, resulting in a larger number of significantly-stressed large domains. The correlations accelerate the spatial smoothing of the fluctuations, culminating in a rupture with a size on the order of the system's size, and representing the final state in which earthquakes occur. Numerical and empirical evidence for this picture indicates that, similar to critical phenomena, the correlation length of the stress-field fluctuations increases significantly before a large earthquake.

Notwithstanding the advances that have been made, the concept of a critical earthquake concept remains only a working hypothesis: from an empirical point of view, the reported analyses possess significant deficiencies and a full statistical analysis establishing the confidence level of the hypothesis remains to be performed. In this vain, Zoller *et al.* [36] and Zoller and Hainzl [37, 38] recently performed novel and systematic spatio-temporal tests of the critical point hypothesis for large earthquakes based on the quantification of the predictive power of both the predicted accelerating moment release and the growth of the spatial correlation length, hence providing fresh support to the concept.

In order to prove, or refute, the notion that a boundary between tectonic plates is a truly critical system, one must check the existence or absence of a build-up of cooperativity prior to a large event in terms of cumulative (Benioff) strain. This means that one should make direct measurements of the stress field and its evolution in space and time in the region in which a large

earthquake is expected, compute its spatial correlation function, deduce the spatial correlation length, and show that it increases with time as a power-law which defines a singularity when the earthquake occurs. Unfortunately, such a procedure is, at present, far beyond our technical observational abilities. It is generally believed that large earthquakes nucleate at a depth of about 10-15 km, implying that the stress field and the correlations would have to be measured at such depths in order to yield an unambiguous signature of what is happening. Moreover, the tensorial stress field would have to be measured with a high enough resolution in order to provide evidence of a clear increase of the correlation length. Such measurements are clearly out of reach at present.

A predictive theory of earthquakes should be able to forecast, (1) *when* and (2) *where* they occur in a wide enough region. It should also be able to (3) distinguish a false alarm from a reliable one. In this paper we propose a completely new method for predicting earthquakes which possesses the three features. The method estimates the Markov time scale (MTS) t_M of a seismic time series - the time over which the data can be represented by a Markov process [39, 40, 41, 42, 43, 44, 45]. As the seismic data evolve with the time, so also does t_M. We show that the time evolutioon of t_M provides an effective alarm a short time before earthquakes. The method distinguishes abnormal variations of t_M *before* the arrival of the P-waves, hence providing enough of a warning for triggering a damage/death-avoiding response *prior to* the arrival of the more damaging S-waves. To distinguish a false alarm from a real one, we describe a second new method of analyzing seismic data which provides a complementary method for predicting when an earthquake may happen. An alarm for an earthquake is then accepted when *both* methods indicate *simultaneously* that an earthquake is about to happen.

The paper is organized as follows. In the next section we introduce two different methods for estimating the Markov time scale of seismic data. In section III we show how the concept of the extended self-similarity (ESS) may be used for analyzing seismic time series. A key quantity deduced from the ESS analysis is a time scale T_1 which is able to detect the change in the correlations in the data, even with a small number of data points. Section IV presents the results of the analysis of seismic data for several earthquakes.

2 Analysis of Seismic Time Series as Markov Process

We have developed two methods for analyzing seismic time series as Markov processes and estimating their Markov time scale (MTS) t_M. In what follows we describe the two methods.

Method 1: In this method one first checks whether the seismic data follow a Markov chain and, if so, measures the MTS $t_M(t)$. As is well-known, a given dynamic process with a degree of stochasticity may have a finite or an infinite MTS t_M - the minimum time interval over which the data can be considered as a Markov process. To estimate t_M, we note that a complete characterization of

the statistical properties of stochastic fluctuations of a quantity $x(t)$ requires the numerical evaluation of the joint probability distribution function (PDF) $P_n(x_1, t_1; \cdots; x_n, t_n)$ for an arbitrary n, the number of the data points in the time series $x(t)$. If $x(t)$ is a Markov process, an important simplification is made as P_n, the n-point joint PDF, is generated by the *product* of the conditional probabilities $P(x_{i+1}, t_{i+1}|x_i, t_i)$, for $i = 1, \cdots, n-1$. A necessary condition for $x(t)$ to be a Markov process is that the Chapman-Kolmogorov (CK) equation,

$$P(x_3, t_3|x_1, t_1) = \int \mathrm{d}(x_2)\; P(x_3, t_3|x_2, t_2)\; P(x_2, t_2|x_1, t_1)\;, \tag{1}$$

should hold for any value of t_2 in the interval $t_3 < t_2 < t_1$. Hence, one should check the validity of the CK equation for various x_1 by comparing the directly-computed conditional probability distributions $P(x_3, t_3|x_1, t_1)$ with the ones computed according to right side of Eq. (1). The simplest way of determining t_M for stationary or homogeneous data is the numerical computation of the quantity, $S = |P(x_3, t_3|x_1, t_1) - \int \mathrm{d}x_2 P(x_3, t_3|x_2, t_2)\, P(x_2, t_2|x_1, t_1)|$, for given x_1 and x_3, in terms of, for example, $t_2 - t_1$ (taking into account the possible numerical errors in estimating S). Then, $t_M = t_2 - t_1$ for that value of $t_2 - t_1$ for which S vanishes or is nearly zero (achieves a minimum).

Method 2: In second method the MTS is estimated using the least square test. The exact mathematical definition of the Markov process is given by [46], by

$$P(x_k, x_k|x_{k-1}, t_{k-1}; \cdots; x_1, t_1; x_0, t_0)$$

$$= P(x_k, t_k|x_{k-1}, t_{k-1}). \tag{2}$$

Intuitively, the physical interpretation of a Markov process is that, it is a process with no memory; it "forgets its past." In other words, only the most nearby conditioning, say (x_k, t_k), is relevant to the probability of finding the system at a particular state x_k at time t_k. Thus, the ability to predict the value of $x(t)$ at time t is not enhanced by knowing its values in steps prior to the the most recent one. Therefore, an important simplification that can be made for a Markov process is that, a conditional multivariate joint PDF can be written in terms of the products of the simple two-parameter conditional PDFs [46] as Eq.(3)

$$P(x_k, t_k; x_{k-1}, t_{k-1}; \cdots; x_1, t_1|x_0, t_0)$$

$$= \prod_{i=1}^{k} P(x_i, t_i|x_{i-1}, t_{i-1}). \tag{3}$$

Here, we use the least square method to estimate the MTS of the fluctuations in the seismic data. Testing Eq.(3) for large values of k is beyond the

present computational capability. However, for $k = 3$, where we have three points, the relation,

$$P(x_3, t_3|x_2, t_2; x_1, t_1) = P(x_3, t_3|x_2, t_2), \tag{4}$$

should hold for any value of t_2 in the interval $t_1 < t_2 < t_3$.

A process is Markov if equation (4) is satisfied for a *certain* time separation, with the MTS t_M being, $t_M = t_3 - t_2$. To measure the MTS we use a fundamental theory of probability that allows us to write any three point PDF in terms of conditional probability functions as,

$$\begin{aligned} &P(x_3, t_3; x_2, t_2; x_1, t_1) \\ &= P(x_3, t_3|x_2, t_2; x_1, t_1)P(x_2, t_2; x_1, t_1). \end{aligned} \tag{5}$$

Using the Markov Processes' properties, and substituting (5), we obtain,

$$\begin{aligned} &P_{Markov}(x_3, t_3; x_2, t_2; x_1, t_1) \\ &= P(x_3, t_3|x_2, t_2)P(x_2, t_2; x_1, t_1). \end{aligned} \tag{6}$$

We then compute the deviations of P_{Markov} from that given by (5), using the least square method:

$$\begin{aligned} \chi^2 = &\int dx_3 dx_2 dx_1 \times \\ &\frac{[P(x_3, t_3; x_2, t_2; x_1, t_1) - P_{Markov}(x_3, t_3; x_2, t_2; x_1, t_1)]^2}{\sigma^2 + \sigma^2_{Markov}} \end{aligned} \tag{7}$$

where $\sigma^2 + \sigma^2_{\text{Markov}}$ are the variance of the terms in the nominator. One should then plot the reduced χ^2, $\chi^2_\nu = \frac{\chi^2}{\mathcal{N}}$, ($\mathcal{N}$ is the number of degrees of freedom), as a function of time scale $t_3 - t_2$. The MTS is that value of $t_3 - t_2$ at which χ^2_ν is minimum.

Our analysis of seismic data (see below) indicates that the average t_M for the *uncorrected* background seismic time series is much smaller than that for data close to an impending earthquake. Thus, at a certain time before an earthquake, t_M rises significantly and provides an alarm for the earthquake. As we show below, the alert time t_a is on the order of hours, and depends on the earthquake's magnitude M and the epicenter's distance d from the data-collecting station(s).

The sharp rise in t_M at the moment of alarm is, in some sense, similar to the increase in the correlation length ξ of the stress-field fluctuations in the critical phenomena theories of earthquake, since t_M is also the time over which the events leading to an earthquake are correlated. Therefore, just as the correlation length ξ increases as the catastrophic rupture develops, so also

does t_M. However, whereas it is exceedingly difficult to directly measure ξ, t_M is computed rather readily. Moreover, whereas ξ is defined for the *entire* rupturing system over long times, t_M is computed *online* (in real time), hence reflecting the correlations of the most recent events that are presumably most relevant to an impending earthquake.

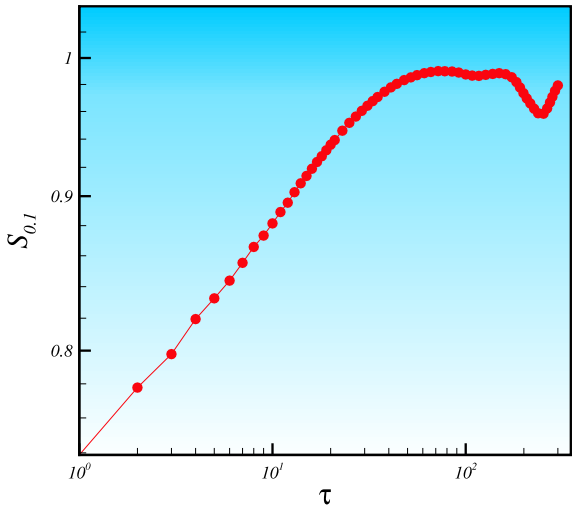

Fig. 1. The structure function $S_{0.1}$ against τ for a typical seismic time series, indicating that the scaling region is small and less than one order of magnitude variations in τ.

3 The Extended Self-Similarity of Seismic Data

To distinguish a false alarm that might be indicated by t_M from a true one, we have developed a second time-dependent function, which is compute based on the extended self-similarity (ESS) of the seismic time series [47, 48]. This concept is particularly useful if the time series for seismic data fluctuations (or other types of time series) do not, as is often the case, exhibit scaling over a broad interval. In such cases, the time interval in which the structure function of the time series, i.e.,

$$S_q(\tau) = \langle |x(t+\tau) - x(t)|^q \rangle \ , \tag{8}$$

behaves as

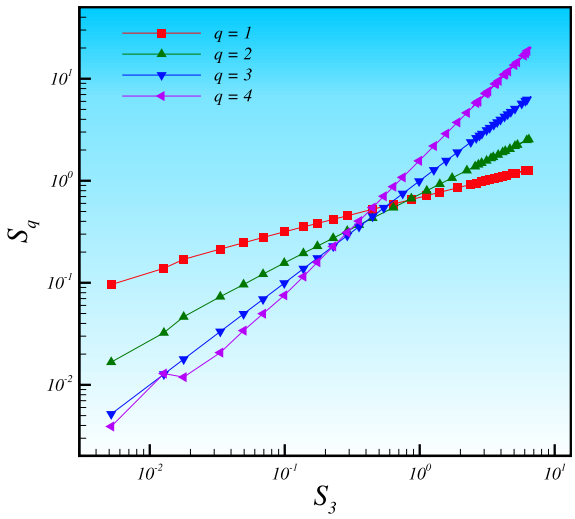

Fig. 2. Generalized scaling analysis of a seismic time series. The structure functions S_q are displayed versus S_3 in the log-log scale.

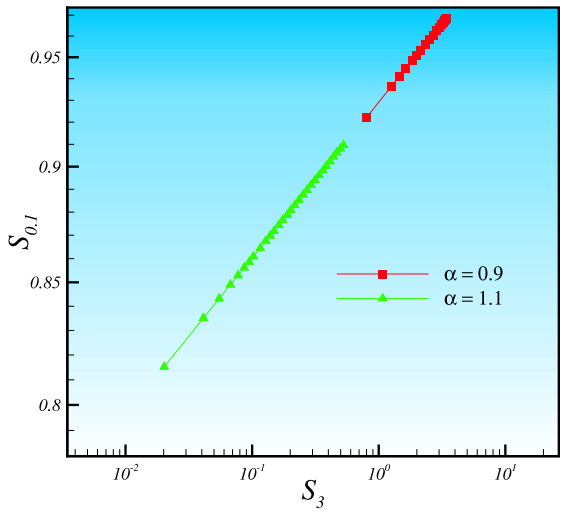

Fig. 3. The structure function $S_{0.1}$ against $S_3(\tau)$ for two type of time series with different scaling exponents.

$$S_q(\tau) \sim \tau^{\xi_q} \ , \tag{9}$$

is small, in which case the existence of scale invariance in the data can be questioned. In Figure 1 the logarithmic plot of the structure function $S_{0.1}(\tau)$ versus τ for a typical set of data with small scaling region is shown. In such cases, instead of rejecting outright the existence of scale invariance, one must first explore the possibility of the data being scale invariant via the concept of ESS. The ESS is a powerful tool for checking multifractal properties of data, and has been used extensively in research on turbulent flows. Thus, when analyzing the seismic time series, one can, in addition to the τ-dependence of the structure function, compute a generalized form of scaling using the ESS concept. In many cases, when the structure functions $S_q(\tau)$ are plotted against a structure function of a specific order, say $S_3(\tau)$, an extended scaling regime is found according to [47, 48],

$$S_q(\tau) \sim S_3(\tau)^{\zeta_q} \ . \tag{10}$$

Clearly, meaningful results are restricted to the regime where S_3 is *monotonic.* For any Gaussian process the exponents ζ_q follow a simple equation,

$$\zeta_q = \frac{1}{3} q \ . \tag{11}$$

Therefore, systematic deviation from the simple scaling relation, (11), should be interpreted as deviation from monofractality. An additional remarkable property of the ESS is that it holds rather well even in situations when the ordinary scaling does not exit, or cannot be detected due to small scaling range, which is the case for the data analyzed here. In Figure 2 we plot the behavior structure function S_q for $q = 2 - 6$ verses the the third moment. It is evident the scaling region is at least two order of magnitude.

It is well-known that the moments with $q < 1$ and $q > 1$ are related, respectively, to the frequent and rare events in the time series [47, 48]. Thus, for the seismic time series one may also be interested in the frequent events in signal. In Figure 3 we show the results for the moment $q = 0.1$ against a third-order structure function for two types of synthetics data with scaling exponent $\alpha = 0.9$ and $\alpha = 1$. The exponent α is related to the exponent of spectral density β, i.e., $S(f) \sim 1/f^{\beta}$, via, $\beta = 2\alpha - 1$. As shown in Figure 3, the interesting feature is that the starting point of $S_{0.1}(\tau)$ versus $S_3(\tau)$ is different for the data for different types of correlation exponents. To determine the distance form the origin, we define [47, 48],

$$T(\tau = 1) = [S_q^2(\tau = 1) + S_3^2(\tau = 1)]^{1/2} \ . \tag{12}$$

Our analysis indicates that since prior to an earthquake the number of frequent events (development of cracks that join up) suddenly rises, one also obtains a corresponding sudden change in S_p with $p < 1$ (we use p=0.1). Close to an earthquake the function $T_1(t)$, also estimated online, suddenly changes

and provides a second alert. Its utility is not only due to the fact that it provides a means of distinguishing a false alarm from a true one indicated by t_M, but also that it is estimated very accurately even with very few data points, say 50, hence enabling online analysis of the data collected over intervals of about 1 second. Thus, even with few data points, the method can detect the change of correlations in the incoming data. For example, for the correlated synthetic data with a spectral density $1/f^{2\alpha-1}$, one obtains, $T_1 = -7(\alpha - 1)$.

4 Test of the Method

To test the method described above, we first generated two synthetic data sets with equal averages and variances (zero and unity, respectively), and mixed them together, as shown in Figure 4, by replacing the last 50 data points of the first set with the first 50 points of the second. As Figure 4 indicates, the Markov time scale t_M and T_1 are able to determine the time at which the two data sets asre mixed.

Now we utilize the method for analyzing seismic time series. We have analyzed the data for *vertical ground velocity* $V_z(t)$ for 173 earthquakes with magnitudes $3.2 \leq M \leq 6.3$ that occurred in Iran between 28°N and 40°N latitude, and 47°E and 62.5°E longitude, between January 3 and July 26, 2004. Recorded by 14 stations, the data can be accessed at http://www.iiees.ac.ir/bank/bank_2004.html. The frequency was 40 Hz for 2 of the stations and 50 Hz for the rest. The vertical ground velocity data were analyzed because, with the method described above, they provide relatively long (on the order of several hours) and, hence, useful alarms for the impending earthquakes. Fourty (discrete) data points/second are recorded in the broad-band seismogram for the vertical ground velocity $x(t) \equiv V_z$. To analyze such data and provide alarms for the area for which the data are analyzed, we proceed as follows.

(1) The data are analyzed in order to check whether they follow a Markov chain [the directly-computed $P(x_3, t_3|x_1, t_1)$ must be equal to the right side of Eq.(2)].

(2) The MTS $t_M(t)$ of the data are estimated by the above two methods. When using method 1 described above, for long-enough data series (10^3 data points or more) the function $t_M(t)$ is computed as the point when $S \to 0$, but for shorter series the minimum in S provides estimates of $t_M(t)$. We also utilize method 2 described above to estimate t_M. To carry out such computations, we use 1000 data points in each window for calculating t_M and move 200 data points at each step inside and outside of the window. This means that for the stations with frequency 50, we estimate a t_M every 4 seconds.

(3) $T_1(t)$ is computed for the same data. To compute $S_q(\tau)$ (we used $q = 1/10$) the data $x(t)$ are normalized by their standard deviation, hence making T_1 dimensionless. We calculate the time series T_1 with 200 data points.

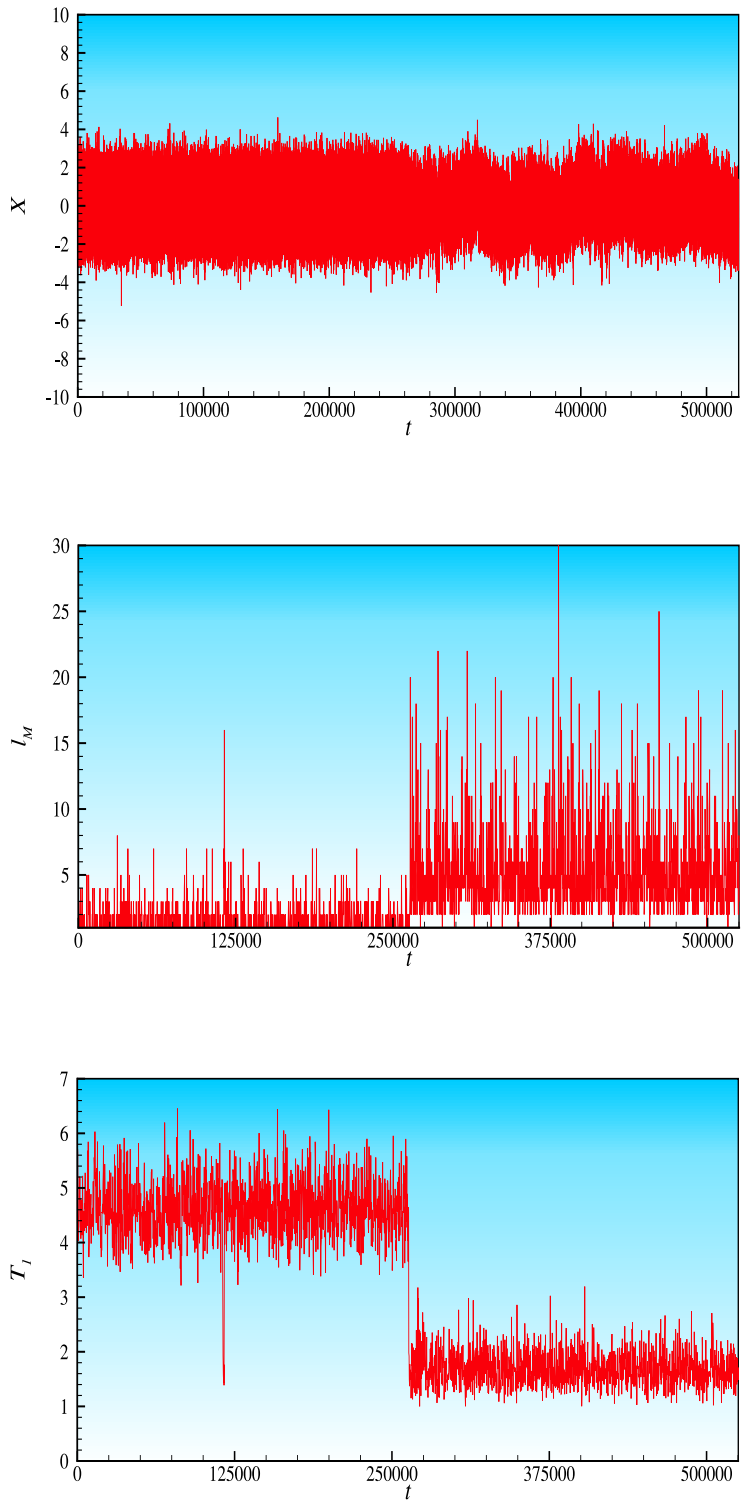

Fig. 4. Mixing of two synthetic time series with different correlation exponent (top); plots of the corresponding t_M (middle), and time variations of T_1 (bottom). As seen, t_M and T_1 distinguish the two types of data.

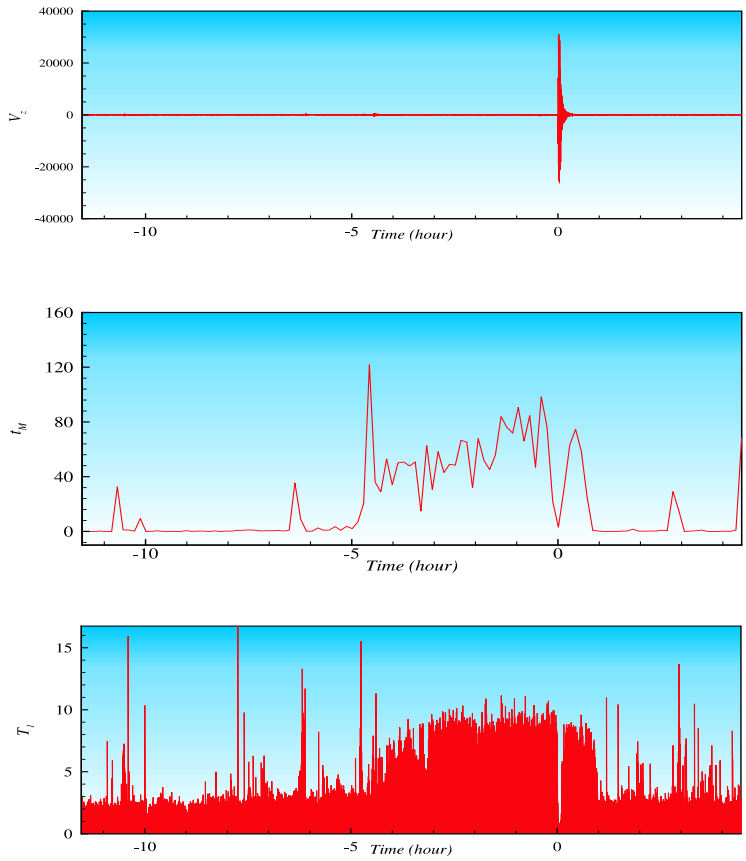

Fig. 5. $T_1(t)$ and $t_M(t)$ for a $M = 5.7$ earthquake that occurred on March 13, 2005, at 03:31:21 am in Saravan at (27.37N, 62.11E, depth 33) in southern Iran. The data were collected at Zahedan station (near Zahedan, Iran) at a distance of ~ 150 km from the epicenter. The earthquake catalogue on the internet address given in the text indicates that, for several days before the main event, there was no foreshock in that region. T_1 and t_M provided a five hour alarm for the earthquake. Since the data used for computing t_M and T_1 were, respectively, in strings of 1000 and 200 points, there is no effect of the events *before* they were collected and, hence, the patterns in the figure reflect the events taking place in the time period in which the data were collected. t_M is in number of data points (the frequency at the station is 40 Hz), T_1 is dimensionless, while $V_z(t)$ is in "counts" which, when multiplied by a factor 1.1382×10^{-3}, is converted to μm/sec. The sensors were (broad-band) Guralp CMG-3T that collect data in the east-west, north-south, and vertical directions. The thresholds are, $t_{Mc} = 10$ and $T_{1c} = 4$.

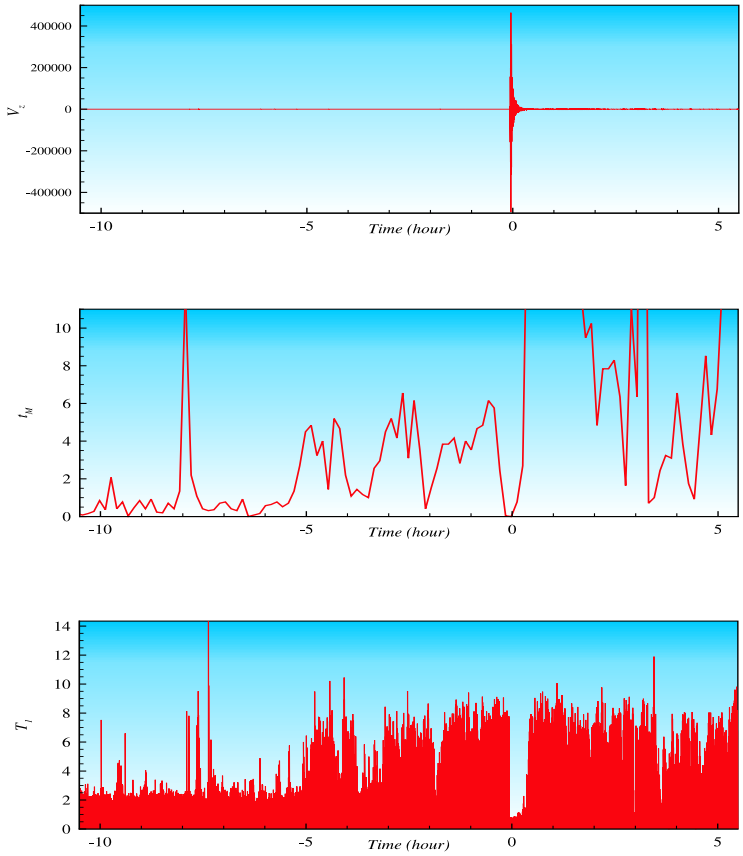

Fig. 6. Same as in Figure 5, but for a $M = 6.5$ earthquake that occurred on February 22, 2005, at 02:25:20 am in Zarand at (30.76N, 56.74E, depth 14) in central Iran. The data were collected at Kerman station (near Kerman, Iran) at a distance of 86 km from the epicenter. The thresholds are, $t_{Mc} = 2$ and $T_{1c} = 4$.

In order to obtain an unambiguous alert from $T_1(t)$, we sometimes calculate the quantity T_1 for the series, $y(t_i) = x(t_i) - x(t_{i-1})$.

(4) Steps (1)-(3) are repeated for a large number of previously-occurred earthquakes of size M at a distance d from the station, referred to as (M, d) earthquakes. Earthquakes with $M < M_c$ and $d > d_c$ are of no practical importance and are ignored.

(5) Define the thresholds t_{Mc} and T_{1c} such that for $t_M > t_{Mc}$ and $T_1 > T_{1c}$ one has an alert for an earthquake $(M > M_c, d < d_c)$. If t_{Mc} and T_{1c} are too large no alert is obtained, whereas one may receive useless alerts if they are too

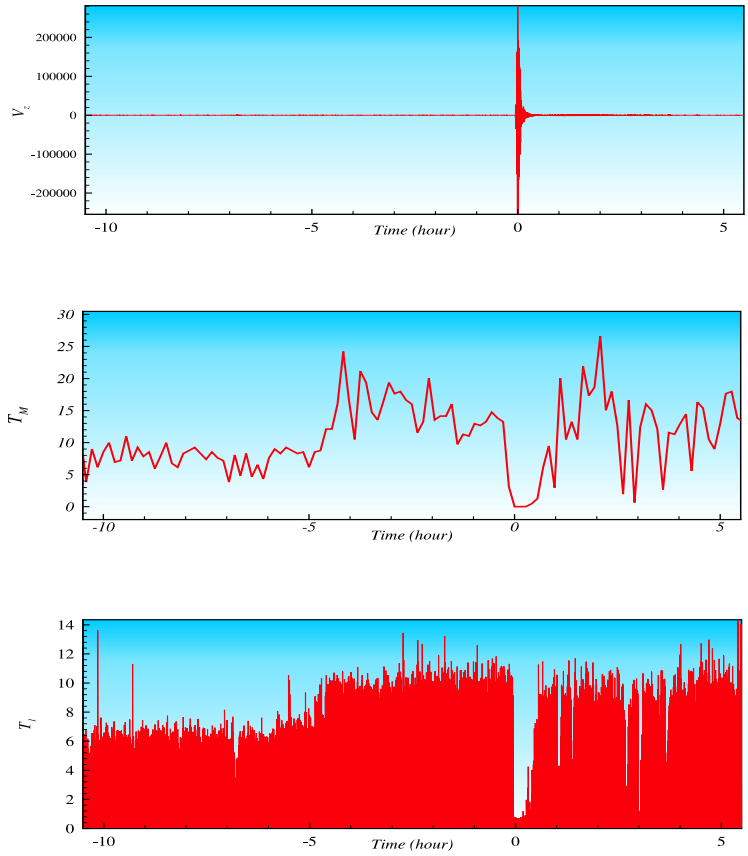

Fig. 7. Same as in Figure 5, but based on the data collected at Ashtian station (near Ashtian, Iran) at a distance of ~ 150 km from the epicenter. Thus, T_1 and t_M provided a about five hour alarm for the earthquake. The thresholds are, $t_{Mc} = 12$ and $T_{1c} = 8$.

small. By comparing the data for all the earthquakes with $M > M_c$ registered in a given station, t_{Mc} and T_{1c} for the earthquakes are estimated.

(6) Real-time data analysis is performed to compute the function $t_M(t)$ and $T_1(t)$. An alarm is turned on if $t_M > t_{Mc}$ and $T_1 > T_{1c}$ *simultaneously*. When the alarm is turned on, it indicates that an earthquake of magnitude $M \geq M_c$ at a distance $d \leq d_c$ is about to occur. The procedure can be carried out for *any* station. The larger the amount of data, the more precise the alarm will be.

Figures 5 presents $T_1(t)$ and $t_M(t)$ for a $M = 5.7$ earthquake that occurred on March 13, 2005 at 03:31:21 am in Saravan at (27.37N, 62.11E, depth 33)

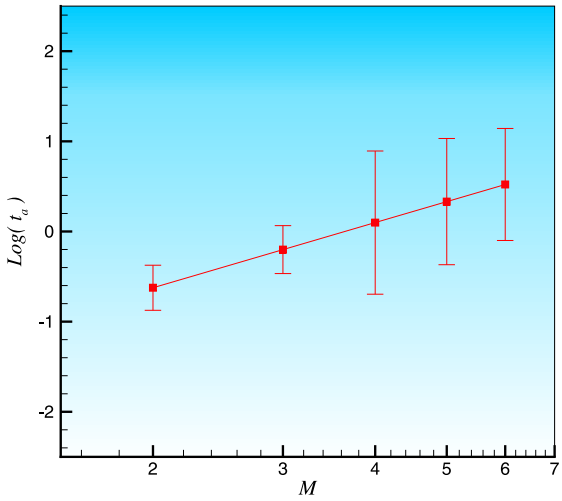

Fig. 8. The dependence of alert time t_a (in hours) on the magnitude M of the earthquakes, obtained based on the data from *broad-band* stations by analyzing 173 earthquakes with magnitudes, $3.2 \leq M \leq 6.3$, that occurred in Iran between 28°N and 40°N latitude, and 47°E and 62.5°E longitude, between January 3 and July 26, 2004.

in southern Iran. The data were collected at Zahedan station (near Zahedan, Iran) at a distance of $\sim$ 150 km from the epicenter. The earthquake catalogue in the internet address given above indicates that, for several days before the main event, there was no foreshock in that region. As Figure 5 indicates, T_1 and t_M provided a five hour alarm for the Saravan earthquake. Since the data used for computing t_M and T_1 were, respectively, in strings of 1000 and 200 points, there is no effect of the events *before* they were collected and, hence, the patterns in Figure 5 reflect the events taking place in the time period in which the data were collected. The thresholds used are, $t_{Mc} = 10$ and $T_{1c} = 4$.

Figures 6 presents $T_1(t)$ and $t_M(t)$ for a $M = 6.5$ earthquake that occurred on February 22, 2005 at 02:25:20 am in Zarand at (30.76N, 56.74E, depth 14) in central Iran. The data were collected at Kerman station (near Kerman, Iran) at a distance of 86 km from the epicenter. All the statements made above regarding the Saravan earthquake are equally true about the Zarand earthquake. Similar to Saravan earthquake, T_1 and t_M provided a five hour alarm for the earthquake. The thresholds used are, $t_{Mc} = 2$ and $T_{1c} = 4$.

Figures 7 presents $T_1(t)$ and $t_M(t)$ for the same Zarand earthquake, but based on the data from another station, collected at Ashtian station (near Ashtian, Iran) at a distance of $\sim$ 150 km from the epicenter. Once again,

there was no foreshock for several days before the main event. Once again, T_1 and t_M provided a five hour alarm for the earthquake. The thresholds used are, $t_{Mc} = 12$ and $T_{1c} = 8$.

To estimate the alert times t_a, which are on the order of hours, we carried out an analysis of online data for 14 stations in Iran's broad-band network (the sensors are Guralp CMG-3T broad-band), analyzing the vertical ground velocity data. Our analysis indicates that t_a depends on M, being small for low M, but quite large for large M. Using extensive data for the Iranian earthquakes with $M \geq 4.5$ and $d \leq 150$ km, we have obtained an approximate relation for the broad-band stations, shown in Figure 8 and represented by

$$\log t_a = -1.35 + 2.4 \log M \ , \tag{13}$$

where t_a is in hours. The numerical coefficients of Eq. (13) for each area should be estimated from the data collected for that area. The above analysis can clearly be extended to all the stations around the world. This is currently underway for Iran's network of stations. For an earthquake of magnitude $M = 4.5$, Eq.(13) predicts an alert time of about 2 hours. Thus, if, for example, three hours after the alarm is turned on, the earthquake has still not happened, we know that the magnitude of the impending earthquake is $M \geq 5.7$.

5 Summary

In summary, we have proposed a new method for analyzing seismic data and making predictions for when an earthquake may occur with a magnitude $M \geq M_c$ at a distance $d \leq d_c$ from a station that collects seismic data. The method is based on computing the Markov time scale t_M, and a quantity T_1 calculated based on the concept of extended self-similarity of the data, and monitoring them *online* as they evolve with the time. If the two quantities exceed their respective critical thresholds t_{cM} and T_{c1}, estimated based on analyzing the data for the previously-occurred earthquakes, an alarm is turned on.

We are currently utilizing this method for Iran's stations. To do so, we calibrate the method with the data for the stations in one region (i.e., estimate t_{cM} and T_{c1} for distances $d < d_c$). If in a given region there is a single station, then once the online-computed t_M and T_1 exceed their critical values, the alarm is turned on. If there are several stations, then once they declare that their t_M and T_1 have exceeded their thresholds, the alarm is turned on. If after about 2 hours, no earthquake has occurred yet, then we know that the magnitude of the incoming earthquake will be greater $M_c = 4.5$ at a distance $d < d_c$.

In fact, over the past two years, the method has been utilized in the Iranian stations. Our analysis indicates that the method's failure rate decreases to essentially *zero* when t_M and T_1 provide *simultaneous* alarms. That is, practically every earthquake that we have considered, including those that

have been occurring while we have been performing online analysis of their incoming data and providing alarms for them (with $M > M_c$), was preceded by an alarm. Of all the earthquakes that we have analyzed so far, the method has failed in only *two* cases. In our experience, if after 10 hours [see Eq. (13)] no earthquake occurs, we count that as a failed case. However, as mentioned, we have so far had only two of such cases.

So far, in order to locate the forthcoming earthquake, we have been using the clustering method which means that, for the area in which three stations are in the alert situation, we can determine the approximate location. However, this can be done using the localization property of seismic waves [49, 50]. We will report the method for the location and precise estimation of the magnitude of forthcoming earthquakes hours before their occurence elsewhere.

Finally, it must be pointed out that the most accurate alarms are obtained from stations that receive data from depths of > 50 m, and are perpendicular to the active faults that cause the earthquake, since they receive much more correlated data for thedevelopment of the cracks than any other station.

6 Acknowledgments

We are particulary grateful to K.R. Sreenivasan, R. Mansouri, S. Sohrabpour and W. Nahm for useful discussions, comments, and encouragement. We would also like to thank M. Akhavan, F. Ardalan, H. Arfaei, J. Davoudi, R. Friedrich, M. Ghafori-Ashtiany, S. Ghasemi, M.R. Ghaytanchi, N. Hamadani, K. Hesami, N. Kamalian, V. Karimipour, A. Mahdavi, S. Moghimi Araghi, N. Nafari, A.F. Pacheco, S. Rahvar, M. Rezapour, A. Sadid Khoy, J. Samikmi, F. Shahbazi, J. Samimi, H.R. Siahkoohi, N. Taghavinia, and M. Tatar for useful comments.

References

1. C.H. Scholz, *The Mechanics of Eathquakes and Faulting* (Cambridge University Press, Cambridge, 1990);
2. V.I. Keilis-Borok and A.A. Soloviev, *Nonlinear Dynamics of the Lithosphere and Earthquake Prediction* (Springer, Heidelberg, 2002).
3. D. Sornette, *Critical Phenomena in Natural Sciences*, 2nd ed. (Springer, Berlin, 2004).
4. L.M. Jones and P. Molnar, J. Geophys. Res. **84**, 3596 (1979).
5. V.I. Keilis-Borok and L.N. Malinovskaya, J. Geophys. Res. **69**, 3019 (1964).
6. G.A. Sobolev and Y.S. Tyupkin, Phys. Solid Earth **36**, 2, 138 (2000).
7. L. Knopoff, *et al.*, J. Geophys. Res. **101**, 5779 (1996).
8. D. Vere-Jones, Math. Geol. **9**, 407 (1977).
9. C.J. Allègre, J.L. Le Mouel, and A. Provost, Nature **297**, 47 (1982);

10. D. Stauffer and A. Aharony, *Introduction to Percolation Theory*, 2nd ed. (Taylor and Francis, London, 1994); M. Sahimi, *Applications of Percolation Theory* (Taylor and Francis, London, 1994).
11. M. Sahimi, M.C. Robertson, and C.G. Sammis, Phys. Rev. Lett. **70**, 2186 (1993); H. Nakanishi, M. Sahimi, *et al.*, J. Phys. I. France **3**, 733 (1992); M.C. Robertson, C.G. Sammis, M. Sahimi, and A.J. Martin, J. Geophys. Res. B **100**, 609 (1995).
12. P.J. Reynolds, W. Klein, and H.E. Stanley, *Phys. Rev. B* (1980).
13. R.F. Smalley, D.L. Turcotte, and S.A. Sola, J. Geophys. Res. **90**, 1884 (1985).
14. M. Sahimi, M.C. Robertson, and C.G. Sammis, *Phys. Rev. Lett.* **70**, 2186 (1993).
15. H. Nakanishi, M. Sahimi, M.C. Robertson, C.G. Sammis, and D. Rintoul, *J. Phys. I. France* **3**, 733 (1992).
16. M.C. Robertson, C.G. Sammis, M. Sahimi, and A.J. Martin, *J. Geophys. Res. B* **100**, 609 (1995).
17. A. Sornette and D. Sornette, Tectonophys. **179**, 327 (1990).
18. B. Voight, *Nature* **332**, 125 (1988); *Science* **243**, 200 (1989).
19. L.R. Sykes and S. Jaumé, *Nature* **348**, 595 (1990).
20. C.G. Bufe and D.J. Varnes, *J. Geophys. Res.* **98**, 9871 (1993).
21. D. Sornette and C.G. Sammis, J. Phys. I. France **5**, 607 (1995).
22. W.I. Newman, D.L. Turcotte, and A.M. Gabrielov, Phys. Rev. E **52**, 4827 (1995);
23. H. Saleur, C.G. Sammis, and D. Sornette, J. Geophys. Res. **101**, 17661 (1996).
24. H. Saleur, C.G. Sammis, and D. Sornette, *Nonlinear Proc. Geophys.* **3**, 102 (1996).
25. A. Johansen, *et al.*, *J. Phys. I France* **6**, 1391 (1996).
26. A. Johansen, H. Saleur, and D. Sornette, *Eur. Phys. J. B* **15**, 551 (2000).
27. M. Sahimi and S. Arbabi, Phys. Rev. Lett. **77**, 3689 (1996).
28. Y. Huang, H. Saleur, C.G. Sammis, and D. Sornette, Europhys. Lett. **41**, 43 (1998).
29. D.D. Bowman, G. Ouillon, C.G. Sammis, A. Sornette, and D. Sornette, J. Geophys. Res. **103**, 2435 (1998).
30. D.J. Brehm and L.W. Braile, Bull. Seism. Soc. Am. **88**, 564 (1998); **89**, 275 (1999).
31. G. Ouillon and D. Sornette, Geophys. J. Int. **143**, 454 (2000);
32. A. Johansen and D. Sornette, Eur. Phys. J. B **18**, 163 (2000).
33. P. Mora, *et al.*, in *Geocomplexity and the Physics of Earthquakes*, edited by J.B. Rundle, D.L. Turcotte, and W. Klein (American Geophysical Union, Washington, 2000).
34. P. Mora and D. Place, *Pure Appl. Geophys.* (2002).
35. D.D. Bowman and G.C.P. King, Geophys. Res. Lett. **28**, 4039 (2001);
36. G. Zoller and S. Hainzl, Geophys. Res. Lett. **29**, 101029/2002GL014856 (2002).
37. G. Zoller and S. Hainzl, *Natural Hazards and Earth System Sciences* **1**, 93 (2001).
38. G. Zoller and S. Hainzl, *Geophys. Res. Lett.* **29**, 101029/2002GL014856 (2002).
39. R. Friedrich and J. Peinke, *Phys. Rev. Lett.* **78**, 863 (1997).
40. R. Friedrich, J. Peinke, and C. Renner, *Phys. Rev. Lett* **84**, 5224 (2000).
41. M. Siefert, A. Kittel, R. Friedrich, and J. Peinke, *Europhys. Lett.* **61**, 466 (2003).
42. M. Davoudi and M.R. Rahimi Tabar, *Phys. Rev. Lett.* **82**, 1680 (1999).

43. G.R. Jafari, S.M. Fazlei, F. Ghasemi, S.M. Vaez Allaei, M.R. Rahimi Tabar, A. Iraji Zad, and G. Kavei, *Phys. Rev. Lett.* **91**, 226101 (2003).
44. F. Ghasemi, J. Peinke, M. Sahimi, and M.R. Rahimi Tabar, *Eur. Phys. J. B* **47**, 411 (2005).
45. M.R. Rahimi Tabar, F. Ghasemi, J. Peinke, R. Friedrich, K. Kaviani, F. Taghavi, S. Sadeghi, G. Bijani, and M. Sahimi, *Comput. Sci. Eng.*, in press (2006).
46. H. Risken, *The Fokker-Planck Equation* (Springer, Berlin, 1984).
47. R. Benzi, *et al.*, *Physica D* **96**, 162 (1996).
48. A. Bershadskii and K.R. Sreenivasan, *Phys. Lett. A* **319**, 21 (2003).
49. F. Shahbazi, A. Bahraminasab, S.M. Vaez Allaei, M. Sahimi, and M. R. Rahimi Tabar, *Phys. Rev. Lett.* **94**, 165505 (2005).
50. A. Bahraminasab, S.M. Vaez Allaei, F. Shahbazi, M. Sahimi, and M.R. Rahimi Tabar, *Phys. Rev. B* (to be published).